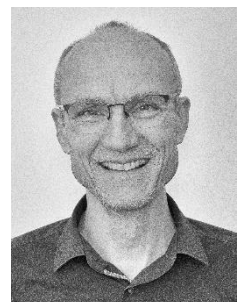


Selbstbohrende Holzschrauben: Einschraubdrehmoment bzw. Auszieh- widerstand und Lageimperfectionen

Matthias Frese
Karlsruher Institut für Technologie
Holzbau und Baukonstruktionen
Karlsruhe, Deutschland



Selbstbohrende Holzschrauben: Einschraubdrehmoment bzw. Auszieh- widerstand und Lageimperfectionen

Dieser Beitrag besteht aus zwei gekürzten Originalaufsätzen, die im Rahmen des *International Network on Timber Engineering Research* 2019 bzw. 2018 vorgestellt wurden. Der erste Teil behandelt Auswirkungen von in Buchenfurnierschichtholz vorhandenen Dichteschwankungen auf Einschraubdrehmomente bzw. Ausziehkräfte von Schrauben (Frese 2019). Es wird darin nachgewiesen, dass solche Schwankungen zu systematischen Unterschieden bei Einschraubdrehmomenten und Ausziehkräften führen. Der zweite Teil stellt Ergebnisse einer Studie vor, in der Abweichungen zwischen der planmäßigen und tatsächlichen Schraubenachse von in Fichtenbrettschichtholz eingebrachten Schrauben untersucht wurden (Frese und Jordan 2018). Die Untersuchungsergebnisse zeigen für einige typische Einschraubsituationen, welche Lageimperfectionen zu berücksichtigen sind, um Kollisionen zwischen Schrauben weitgehend auszuschließen.

1. Density variations in beech LVL - influence on insertion moment and withdrawal capacity of screws

1.1. Motivation and objective

The manufacturing process of beech LVL panels causes panel to panel and inherent density variations. Unlike panel to panel variation, where the density changes from one panel to another, inherent variations arise perpendicular to the veneer layers in the cross-section of a single panel in a narrow area. If panels are processed to glulam-like products, inherent variations repeat in every lamination. Density variations in turn influence amongst others the insertion moment and the withdrawal capacity of self-tapping or self-drilling wood screws. prEN 14592 provides EN 15737 for testing the insertion moment and EN 1382 for testing the withdrawal capacity. Both testing standards apply to engineered wood products too. In both of them, it is generally stipulated that the density of the provided specimens has to be representative for that of the material actually used. However, there is no further reference how to account for specific density variations in wood-based products as beech LVL launched in the market of building materials in 2014 (Hassan and Eisele 2015). For that reason, this study aims at looking into the correlation between such density variations in beech LVL and these parameters. In a broader sense, the findings may contribute to a more purposive and better application of the preceding testing standards in terms of both parameters and LVL-based products. The results presented and discussed hereafter were gained in a research project on the development of self-drilling screws for high dense wood products (Frese and Blaß 2018).

1.2. Causes of density variations in beech LVL

In asking about the causes of density variations in beech LVL, one has to differentiate between panel to panel and inherent variations. A natural reason for both types of variations is the density variation of the beech wood itself or the veneers thereof. Further causes lie in the manufacturing process as illustrated in Fig. 1. In order to manufacture a beech LVL standard panel with a nominal thickness of 40 mm, 14 rotary peeled veneers are fed into a continuous hot press. Prior to the feeding, glue is applied on one of the adjacent veneer faces. At this stage of manufacture, the uncompressed stack is called veneer fan. The veneers are ideally 3.35 mm in thickness resulting in a 47 mm thick unit at the beginning of densification. The following densification process is accompanied by controlled heat supply and compression in radial direction (of the veneers) to achieve a 10% densification of the veneer fan and, finally, a constant panel thickness of 42 mm prior to sanding of both surfaces. If the averaged thickness of all the veneers in the fan is significantly thinner than 3.35 mm, the fan is less densified compared to densification under ideal conditions. If it is significantly thicker, the fan is more densified. Such changes cause the density variations

from panel to panel. This variation is hereafter referred to as V1. Maximum densification takes place at a certain combination of temperature and compression. However, since temperature is not constant both in thickness and manufacturing direction and since compression decreases in manufacturing direction, outer veneers are more strongly densified compared to inner ones. This effect is known as surface densification of wood as described for example by Tarkow and Seborg 1968. As a consequence, the local density systematically varies along the thickness direction of the panel. The manufacturing process causes, therefore, higher local density in the outer layers than in the inner ones. This variation is hereafter referred to as V2. It is to be expected that the density variations V1 and V2 influence mechanical resistances of the material. Depending on the location where a screw is inserted and depending on the direction of insertion one has to be aware of systematic differences in the values of insertion moment and withdrawal capacity of screws.

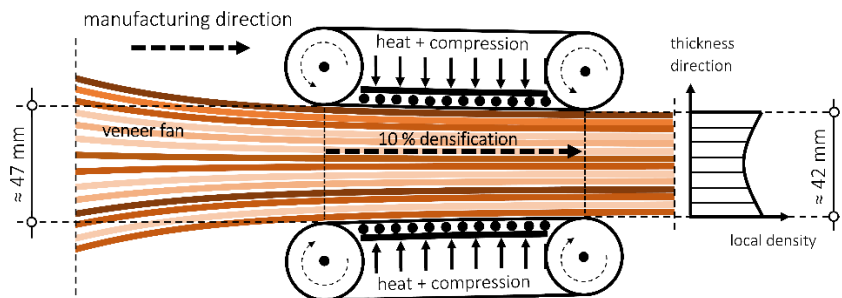


Figure 1: Simplified schematic of the manufacturing process: a veneer fan with glue in the relative interfaces is continuously moved in manufacturing direction under heat supply and compression.

1.3. Examination of density variations

The density variations V1 and V2 were examined. In case of V1, the densities of 160 small cross-sectional slices were determined. The slices originated from different panels or spatially separated panel regions. Each slice was 40 mm thick and, therefore, encompassed 14 veneers. One half of these slices contained two cross layers and was 100 mm wide the other half had no cross layers and was quadratic. Examples of the slices are illustrated in Fig. 2 (left). The single values of the V1 specimens describe a density averaged over the nominal panel thickness $t_{\text{lam}} = 40 \text{ mm}$ with 14 veneers. In case of V2, seven large cross-sectional slices as exemplified in Fig. 2 (middle) were sawn off from glulam-like beams (240 mm in depth) composed of six beech LVL laminations. These slices contained, therefore, five secondary glue lines. The laminations originated from panels with nominal thickness. The slices were separated parallel to the veneer layers into 24 times 6.8 mm thick stripes each as illustrated in Fig. 2 (right). During separation by sawing, the secondary glue lines were carefully preserved in the relative stripes. Afterwards their densities were determined. Hence, the values describe a local density which reflects an average over approximately 7 mm with 2-3 veneer layers.

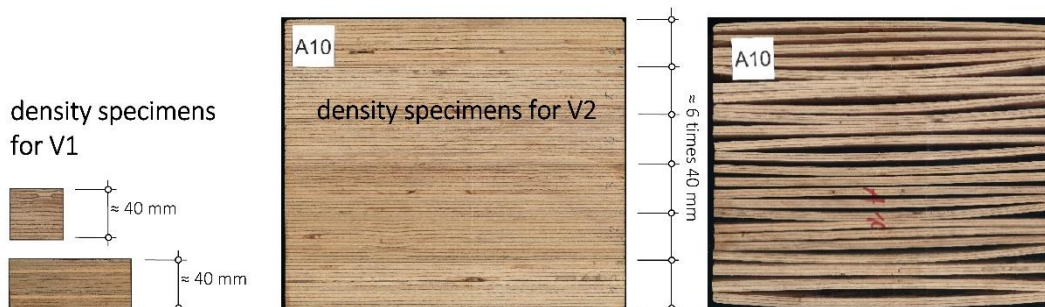


Figure 2: Small cross-sectional slices, slice cut from glulam-like beams and stripes for the density profile.

Fig. 3 shows the probability distributions of the values for V1 and V2. While means are almost similar ($816/802=1,017$), the COV and the span between minimum and maximum values increase with decreasing quantity of veneer layers in the respective unit. In Fig. 4, the local density values are plotted against the respective stripe number in ascending order. Hence, this

representation exemplifies the density profiles perpendicular to the veneer layers or along the glulam beam depth of 240 mm for each of the seven slices. The connecting lines make clear that the typical density profile shown in Fig. 1 (right) actually repeat in every lamination.

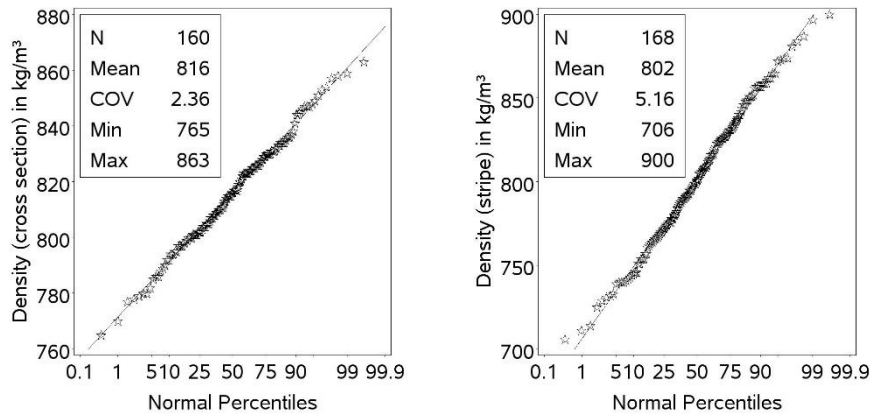


Figure 3: Density variation: panel to panel by small cross-sections (V1) and inherent by stripes (V2).

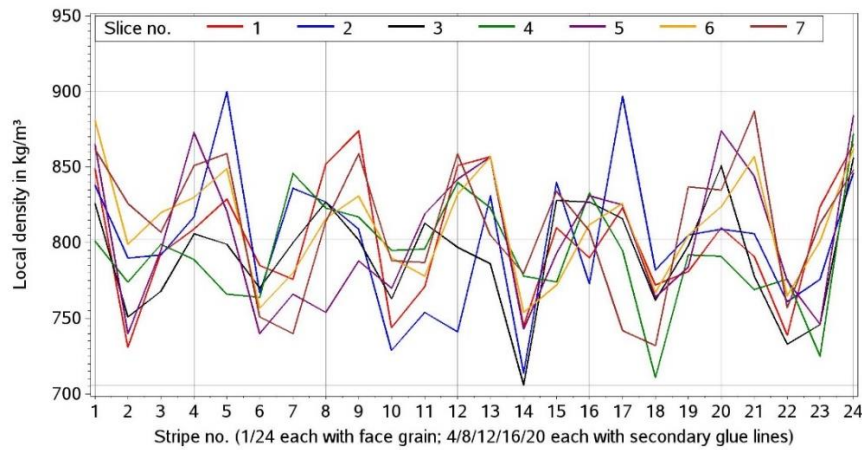


Figure 4: Density profile perpendicular to the veneer layers in glulam-like beech LVL.

1.4. Insertion tests

In total, 664 self-drilling screws (ASSY 3.0) were driven in beech LVL specimens while the torsional moment during insertion (torsional moment) was recorded. The experimental work was carried out by Stieger 2016. Table 1 contains the detailed information on nominal diameter (d) of the screws, their total length, thread length, tip shape and rough thread. The last two columns contain definitions of the examined global insertion directions and positions. In order to figure out any differences between the insertion moments related to the three possible global insertion directions (s. Fig. 5 left) extensive comparative tests were carried out with 7-mm screws. Additionally to that, differences were examined between insertion moments of the two global directions perpendicular to the face and edge grain with 5-mm and 10-mm screws. Using all the screw diameters, insertion tests with staggered positions in the edge grain (as illustrated in Fig. 5 right) were conducted. Thereby, the influence of the inherent density variation between the secondary glue lines was considered.

Table 1: Wood screws and test programme.

d mm	Screw length mm	Thread length mm	Tip shape	Rough thread	Global insertion direction	Staggered insertion in edge grain
5	120	60			face/ - /edge	yes
6	110	70			- / - /edge	yes
7	160	80			face/end/edge	yes
8	220	100			- / - /edge	yes
10	320	120			face/ - /edge	yes

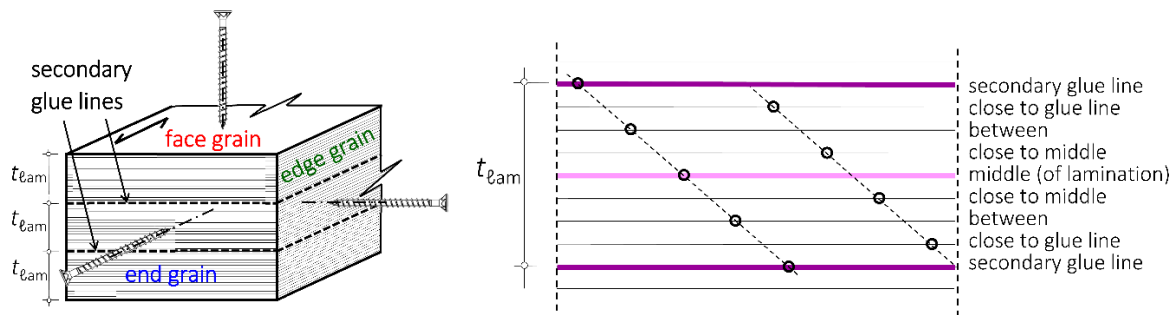


Figure 5: Global insertion directions and staggered insertion positions in the edge grain

1.5. Withdrawal tests

160 withdrawal tests were performed. The experimental work was carried out by Walter 2016. The nominal diameter (d) of the screws varied between 7.2 and 8.5 mm. The pitch and the ratio of core to nominal diameter were also varied. Prior to insertion of the screws, the specimens were predrilled with the core diameter. One half of the screws was inserted perpendicular to the face grain and the other half perpendicular to the edge grain as illustrated in Fig. 6 on the left and right side, respectively. The penetration length was constant and corresponded to 40 mm. In the face grain, both higher and lower densified veneers proportionally contributed to the withdrawal capacity. In the edge grain, the position of the screw axis was exclusively in the middle of a lamination. Thus, their screw channel was in an area where the density of the veneers exhibits the lowest values. The withdrawal parameter (f_{ax}) was evaluated using the maximum testing load and the product of nominal diameter and penetration length.

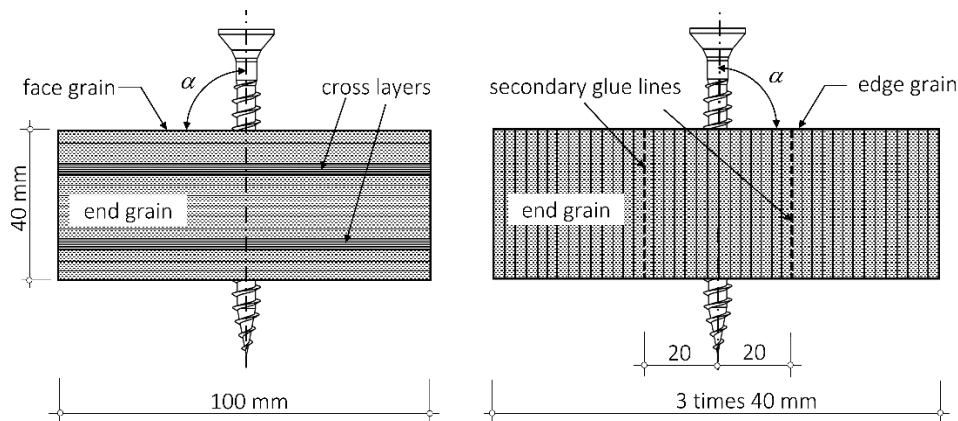


Figure 6: Specimens for the withdrawal tests.

1.6. Results of the insertion and withdrawal tests

Fig. 7 is composed of three diagrams and shows the evaluation of 276 insertion tests with 7-mm screws. For the respective evaluation of 5, 6, 8 and 10-mm screws, see Frese 2019. The diagram at the top makes clear the span of torsional moments depending on the insertion depth and the global insertion direction. For each of the three global directions, the data of the respective curves were put together and were represented by a high low plot procedure where vertical lines show the span and the continuous lines the mean value. The diagram in the middle exemplifies the maximum torsional moments depending on the insertion depth and the global direction. The curves of the maximum torsional moments are not necessarily related to a single insertion test but represent an upper envelope curve. The diagram at the bottom describes the maximum torsional moments depending on insertion depth and the examined staggered positions in the edge grain. In detail, the diagram exemplifies the respective upper envelope curves which were obtained for the five different positions.

The insertion tests give evidence that the largest span of torsional moments arise in the edge grain and the lowest in the face grain. The span of torsional moments in the end grain is larger than that in the face grain, but smaller than that in the edge grain.

Independently of the insertion depth, the maximum torsional moments develop in the edge grain. The differences between the maximum values in the edge grain and those in the face and end grain are very pronounced. The evaluation in Table 2 (upper part) exemplifies these differences in numbers for insertion depths 40 and 80 mm.

Screws systematically driven in the staggered positions in the edge grain exhibit their maximum torsional moments in the following positions: glue line, close to glue line and between. Thus, the torsional moments are correlated with the inherent density variation V_2 to some extent. An evaluation in numbers is shown in Table 2 (lower part). Herein, the differences amount to more than 30%.

Since the rough threads become effective after an insertion depth deeper than the thread length of 80 mm, the curves show a steeper gradient after that depth.

Table 2: Evaluation of maximum torsional moments for 7-mm screws

Direction/position	Depth in mm	$M_{t,max}$ in Nm	Depth in mm	$M_{t,max}$ in Nm
⊥ face grain	40	9.04 (79%)	80	12.3 (77%)
⊥ end grain		8.46 (74%)		12.7 (79%)
⊥ edge grain		11.4 (100%)		16.0 (100%)
middle	40	8.70 (88%)	80	11.7 (83%)
close to middle		8.55 (86%)		12.0 (85%)
between		9.41 (95%)		12.6 (89%)
close to glue line		11.4 (115%)		16.0 (113%)
glue line		9.93 (100%)		14.1 (100%)

There are significant differences between the withdrawal parameters which relate to the two insertion directions (Table 3). In agreement with the correlation found between the torsional moments and faces, the lowest 5th percentile (37.2 N/mm²) was determined for the edge grain in the middle of a lamination. This value amounts to 80% of that found for the face grain (47.3 N/mm²).

Table 3: Statistics of results for withdrawal tests

Withdrawal perp. to	N	f_{ax} in N/mm ²			Density in kg/m ³		
		Mean	COV	5th P.	N	Mean	COV
face grain	77	55.4	8.29	47.3	80	819	25.2
edge grain, middle	77	43.3	9.26	37.2	80	813*	21.4

* Averaged over 14 veneer layers. The mean does not reflect the local density directly around the screw channel.

1.7. Conclusions

Findings concerning density variations and consequences in terms of insertion and withdrawal tests are:

- The accuracy in describing density variations in beech LVL depends on the size of the unit used for the density determination. Outer layers in beech LVL panels exhibit the highest density (about 900 kg/m³), inner ones the lowest (about 700 kg/m³). This is in line with findings of surface densification in engineered wood products manufactured in continuous hot presses.
- In order to obtain the highest torsional moments in beech LVL, screws should be tested in or close to the secondary glue lines in the edge grain of glulam made of beech LVL. In case of new types of LVL products, all faces should be subject of the insertion tests and staggered insertion positions should be examined in the edge grain.
- Screw failure during insertion must not occur. Therefore, a comparison between the actual maximum torsional moments and the characteristic torsional strength may be used to adapt and improve the safety margin in terms of screw failure, cf. EN 14592. Unlike softwoods where high-dense knot clusters randomly occur, influences on the torsional moments in beech LVL and comparable LVL products made of other wood species are more predictable.

- The influence of the inherent density variation on the withdrawal capacity is comparable to that on the torsional moment. Assuming $\alpha = 90^\circ$, the lowest withdrawal capacities are to be expected in the middle of a lamination in the edge grain. Nevertheless, withdrawal tests should be performed in all relevant faces to figure out potential differences between the respective withdrawal parameter. It should be noted that locally slight splitting could also have had an influence on the lower withdrawal capacities of screws inserted in the middle of the lamination.
- Consequences of screw failure during insertion are seen to be critical, since screw failure means total loss of a screw. The withdrawal capacity of a screwed connection is usually based on more than two screws. Hence, a common withdrawal capacity in the edge grain is seen to be less sensitive to inherent density variations.

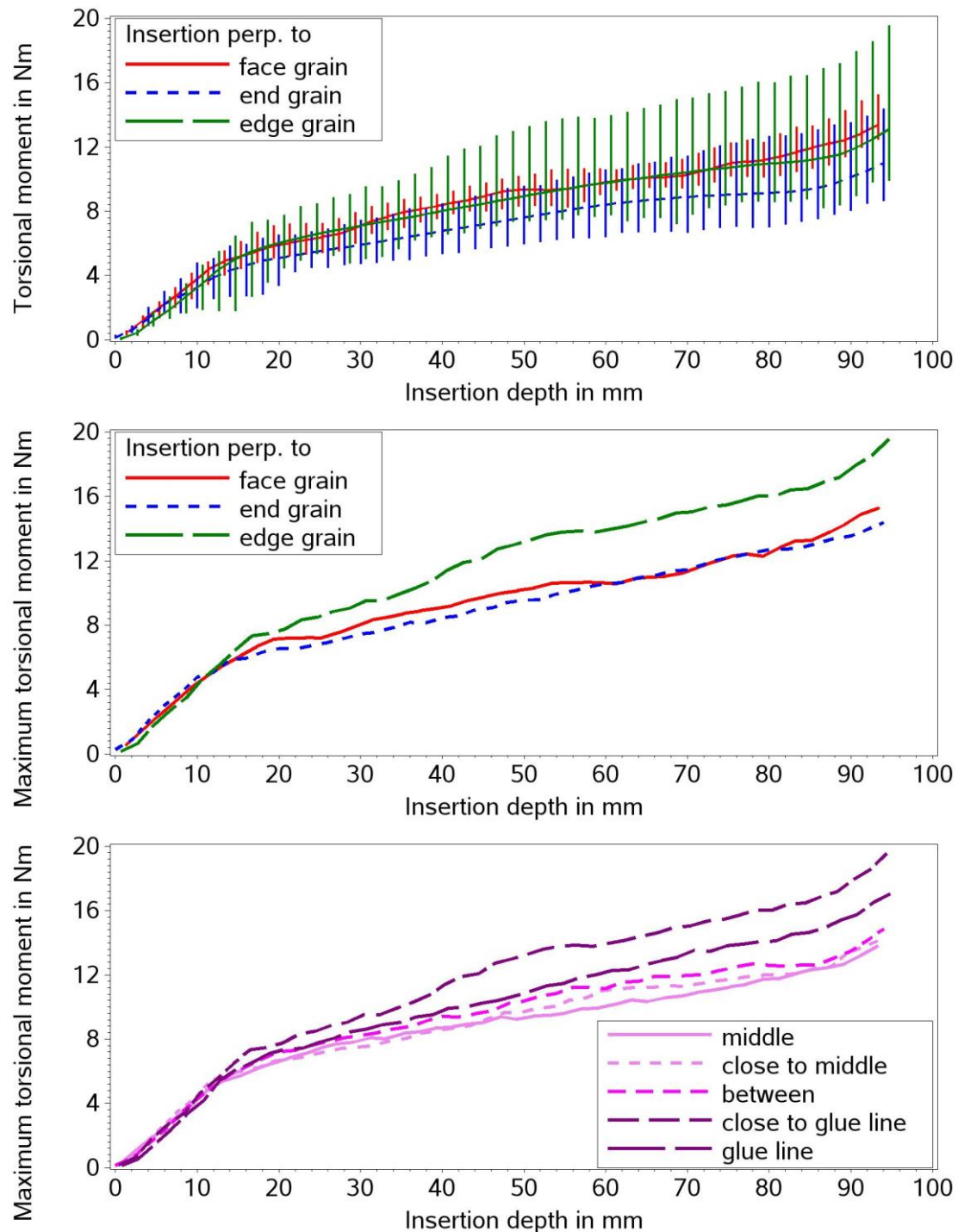


Figure 7: Results for 7-mm screws.

2. Deviations between planned and actual position of wood screws - consequences for minimum spacing

2.1. Motivation and objective

The insertion of self-tapping (self-threading) or self-drilling wood screws is usually accompanied by minor or major deviations between the planned screw axis and the actual one. The actual positions can be seen as a result of an individual insertion process influenced by a complex interaction between multiple parameters. A concise representation of this issue is for example given by Trautz and Koj 2015. They stress amongst others the necessity of sufficient spacing between adjacent screws to avoid contact problems. Occasionally, screw connections comparable to those in Fig. 8 have shown harmful contact between narrow placed screws although minimum spacing was observed in design and execution. The minimum spacing between the represented crossed screw couples is usually given as a multiple (k) of the nominal screw diameter (d).

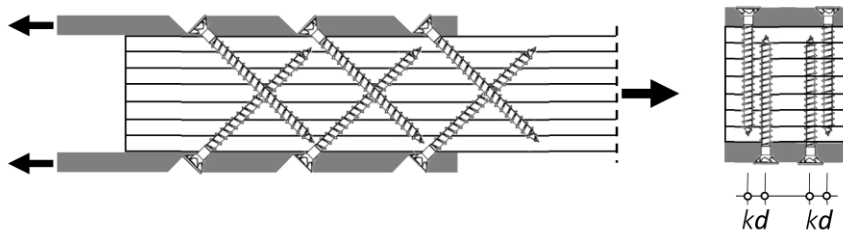


Figure 8: Crossed screw couples with hazard of contact in case of too narrow mutual spacing.

Several European technical assessments stipulate at least 1.5 for k . Eurocode 5 contains the general rules for minimum spacing rules being completed and extended by European technical assessments (ETAs).

Müller 2017 and Blaß 2017 recently reported contact problems with crossing screws. Furthermore, skilled carpenters, practitioners and designers have experienced such contact problems. Fig. 9 shows typical damages to screws of a crossed couple caused by contact. Even in reinforcement measures with long screws for shear and stresses perpendicular to the grain, critical deviations of the actual screw channel occur (Blaß and Krüger 2010). Otherwise, reinforcing techniques based on controlled contact between screws and dowels require very accurate screw placements to ensure the intended load distribution between these components (e.g. Bejtka and Blaß 2005).

These aspects show the necessity to realistically estimate deviations between the planned and actual screw axis. For that purpose, about 350 insertion tests with wood screws were conducted and evaluated in a preliminary study (Jordan 2017). The aims of this study were 1. the identification of some crucial parameters influencing deviations, 2. the experimental determination of such deviations and 3. a proposal for a first tentative model predicting appropriate minimum spacing.



Figure 9: Damages to wood screws caused by mutual contact. Local damage to a firstly screwed-in screw (left) hit by a secondly screwed-in one (right) resulting in almost complete loss of the thread.

2.2. Interaction between insertion and wood structure

Potential parameters influencing deviations between the planned and actual screw axis are amongst others (cf. Trautz and Koj 2015): the technical equipment, the way someone screws in, with/without pre-drilling, use of short pilot holes, insertion angle between screw axis and wood surface (β), shape of the screw tip, straightness of the screw, angle between screw axis and grain direction (α), natural growth characteristics along the screw channel, glue lines,

insertion length (ℓ), wood species, physical wood properties, screw stiffness or even unintended contact with other screws crossing the actual screw channel.

The glulam cube in Fig. 10 exemplifies that a planned screw axis can be described by a vector \vec{a} in the spatial wood structure. Hence, the connection between the screw axis and the glulam structure is defined by a given orientation of the cube in the coordinate system and the coordinates a_x , a_y and a_z defining the screw axis. Using this system, the examined placements of screws in glulam are described below.

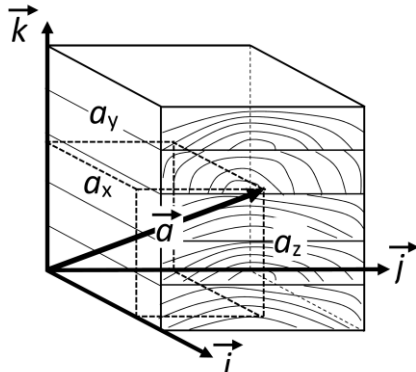


Figure 10: Direction of a planned screw axis by means of the vector \vec{a} .

2.3. Examination of deviations

72 specimens for the insertion tests were made of spruce glulam GL24c. The specimens were realised from four glulam members, each 12 m in length, 180 mm in width and 200 mm in depth. The members consisted of five laminations. Where necessary, specimens were glued together to obtain sufficient dimensions for the intended insertion lengths. The density and the moisture content were measured by means of a cross-sectional slice at one third of the specimens. The results are compiled in Table 4. Table 5 contains the properties of the screws. Crucial variations refer to the screw length (to realise three different insertion lengths), the thread length and the tip shape. The nominal diameter was uniformly 8 mm.

Table 4: Density and moisture content of the glulam specimens.

Glulam property	N	Mean	SD	Min	Max
Density in kg/m ³	21	428	24	388	470
Moisture content in %	21	11.4	0.89	10.4	14.7

Table 5: Wood screws.

Drill tip	d mm	Screw length mm	Thread length mm	Insertion length mm	Tip shape
with	8	220	200	160	
		280	260	220	
		370	350	340	
without	8	220	100	160	
		260	100	220	
		380	100	340	

Four different screw placements (I, II, III and IV) were examined. The corresponding section planes, in which the planned screw axes lie, are visualised in Fig. 11. The vectors of the screw axes and the resulting angles (α) between screw axes and grain direction are quoted in Table 6. The screws were inserted by a single person using a hand-hold electric-powered screwdriver. The holes were neither pre-drilled nor pilot holes were provided. At the beginning of the insertion wedge-shaped screw guides equipped with grooves were used to ensure the intended insertion angle ($\beta=45^\circ$ and 90°) between screw axis and surface as accurately as possible. Up to six screws were inserted in each specimen. Deviations between the planned exit points (E) and the actual ones were measured at the surface of the exit point. The coordinates $\Delta 1$ and $\Delta 2$ defined as orthogonal vectors originating from E were then computed by means of vector calculations. Fig. 11 in total

represents the connection between the planned exit points, the actual ones and the positive directions of the computed coordinates $\Delta 1$ and $\Delta 2$.

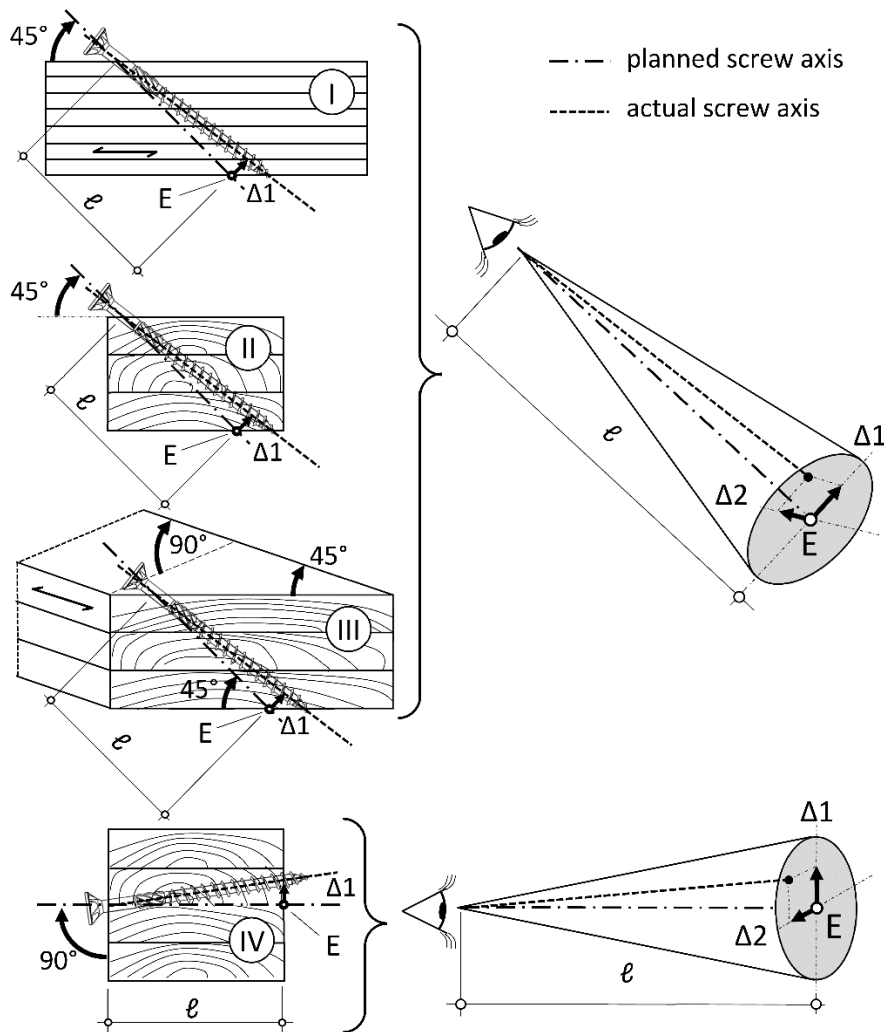


Figure 11: Examined placements

Table 6: Coordinates of the examined vectors \vec{a} .

Placement	a_x	a_y	a_z	\vec{a}	α	β	placement in the..
I	1	0	1	(1,0,1)	45°	45°	longitudinal section
I	1	1	0	(1,1,0)	45°	45°	longitudinal section
II	0	1	1	(0,1,1)	90°	45°	cross-section
III	0.71*	0.71*	1	(0.71,0.71,1)	60°	45°	diagonal section
IV	0	1	0	(0,1,1)	90°	90°	cross-section/glue line

$$* = \sqrt{1/2}$$

2.4. Results for $\Delta 1$ and $\Delta 2$

Fig. 12 shows the results for the placement imperfections I-IV. The diagrams contain the deviations $\Delta 1$ and $\Delta 2$ differentiated by insertion length. Amongst others, these observations were made:

- **Placement I:** $\Delta 1$ is almost exclusively positive (Fig. 12-I). Independent of the insertion length, $\Delta 2$ is more or less symmetrically distributed around the vertical axis with $\Delta 2 = 0$.
- **Placement II:** $\Delta 1$ is almost exclusively positive except for the insertion length of 340 mm (Fig. 12-II). Independent of the insertion length, $\Delta 2$ is more or less symmetrically distributed around the vertical axis with $\Delta 2 = 0$.

- **Placement III:** $\Delta 1$ is exclusively positive; however, screws inserted with 220 mm exhibit also almost exclusively positive $\Delta 2$ values (Fig. 12-III). The distribution of $\Delta 2$ is symmetrical.
- **Placement IV:** The scatter of $\Delta 1$ is larger than the one of $\Delta 2$ (Fig. 12-IV). Independent of the insertion length, both deviations are symmetrically distributed around their corresponding axes with $\Delta = 0$. Only three screws kept their screw channel exactly in the glue line.

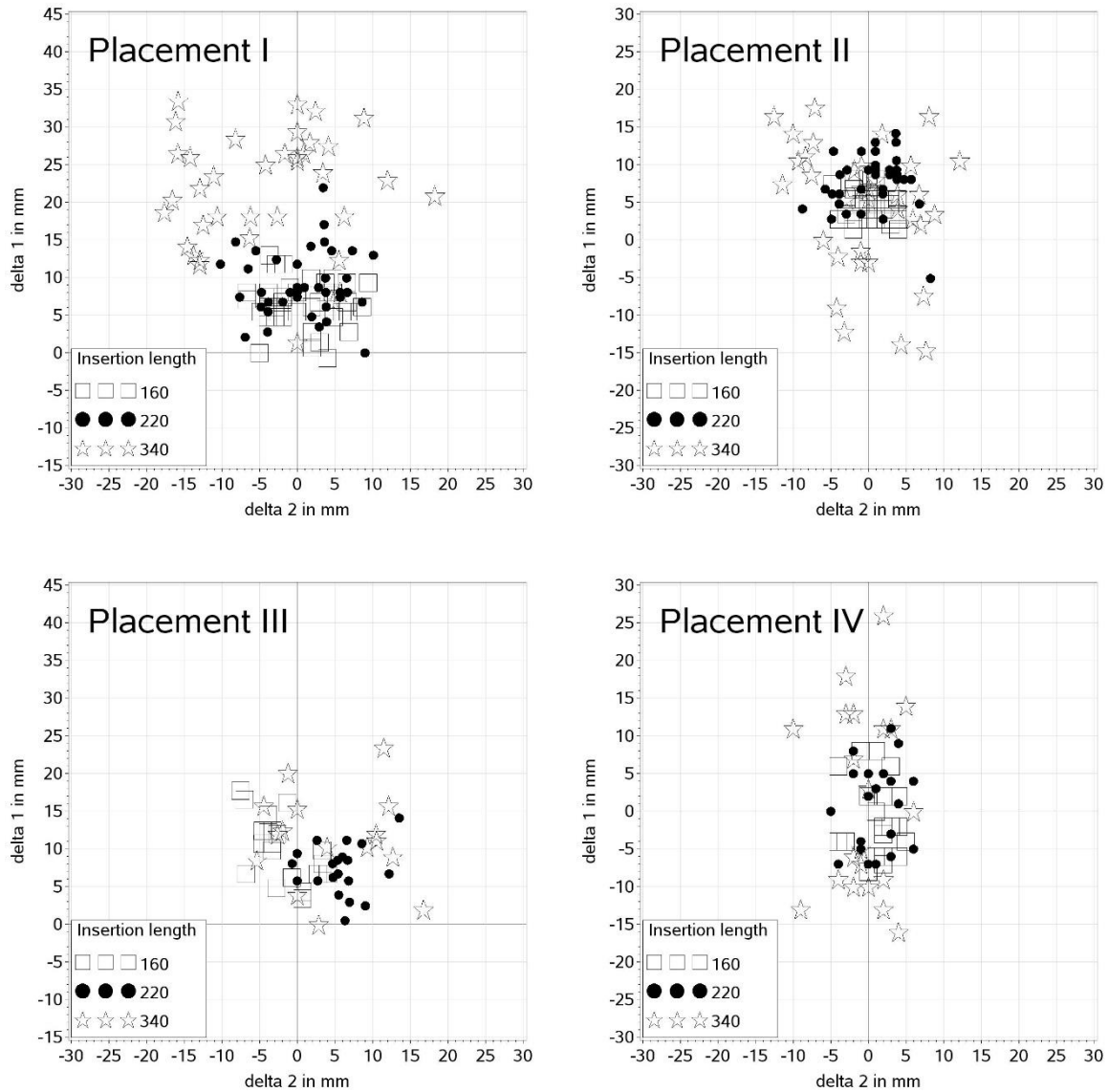


Figure 12: Deviations of placement I-IV.

2.5. Absolute deviation and cone model

Using equation (1) the absolute deviation denoted as radius r was computed. The radius r and the corresponding insertion length yield a deviation angle ε , see equation (2). The maximum of $\tan \varepsilon$ ($\max \tan \varepsilon$) is quoted in Table 7 for the four placements and the corresponding insertion lengths.

$$r = \sqrt{\Delta 1^2 + \Delta 2^2} \quad (1)$$

$$\tan \varepsilon = r/l \quad (2)$$

Table 7: Statistics of the absolute deviation.

Placement	Insertion length mm	N	$r = \sqrt{\Delta 1^2 + \Delta 2^2}$			max $\tan \varepsilon$
			Mean mm	CV %	Max mm	
I	160	41	8.02	33	13.5	0.084
	220	48	10.4	36	22.2	0.101
	340	37	23.8	32	37.1	0.109
II	160	37	5.24	31	8.82	0.055
	220	31	9.17	31	14.6	0.066
	340	30	10.3	50	20.7	0.061
III	160	19	10.7	41	19.3	0.121
	220	20	9.89	33	19.6	0.089
	340	21	13.5	40	26.1	0.077
IV	160	23	5.38	37	8.06	0.050
	220	20	6.09	38	11.4	0.052
	340	21	11.6	45	26.1	0.077
Total:		348 insertion tests				

The placements I/III and II/IV are grouped because of comparable placement conditions and similar magnitude of deviations. Thus, the maximum angles given by $\tan \varepsilon$ are 0.121 and 0.077 for the placement groups I/III and II/IV, respectively. Fig. 13 shows a general cone model. This model would basically be suitable to estimate the cone shaped clear space around a planned screw axis a screw¹ needs to be inserted without having contact with other screws. Based on the presently available data the space should be calculated with $\tan \varepsilon$ of about 0.12 (≈ 0.121) and 0.08 (> 0.077) for the groups I/III and II/IV, respectively. These proposed values for the tangent do not contradict deviations published by Trautz and Koj 2015.

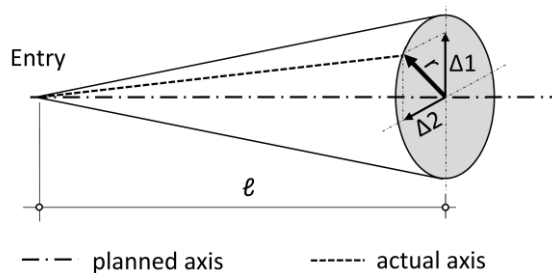


Figure 13: Visualised cone model.

2.6. Proposal for minimum spacing considering stochastic effects

The statistics in Table 8 show that significant differences exist between the upper percentiles of $\tan \varepsilon$ belonging to the corresponding placement groups.

Table 8: Statistics and upper percentiles of $\tan \varepsilon$.

Placement group	N	Mean	SD	95%	99%	Max
I/III	176	0.0542	0.0218	0.0950	0.112	0.121
II/IV	172	0.0339	0.0131	0.0543	0.0665	0.0767

Stochastic effects for group I/III and II/IV (values in brackets) are considered using the 95th percentile. Consequently, the exceedance probability of $\tan \varepsilon = 0.0950$ (0.0543) is less than 5%. Hence, the probability that the unintended tangent of two independent adjacent screws exhibits 0.1 (0.06) is less than 0.25%. Fig. 14 exemplifies that the actual probability of contact between two screws in the critical area is far lower than 0.25% due to the circular distribution² of possible locations after a corresponding large insertion length l_{crit} .

¹ Nominal diameter here assumed as 0

² Uniform circular distribution of locations assumed for simplicity reasons

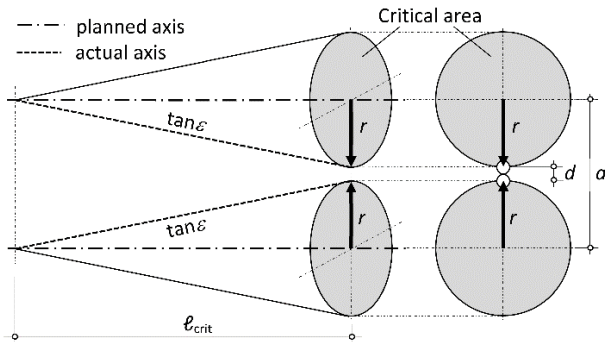


Figure 14: Spacing a between two planned screw axes based on $\tan \varepsilon$, l_{crit} and d .

Equation (3) reflects these considerations. Inserting $\tan \varepsilon = 0.1$ and 0.06 for group I/III and II/IV, respectively, yield the mutual spacing a between two adjacent screws in a critical area.

$$a = 2l_{crit} \cdot \tan \varepsilon + d \quad (3)$$

Favourable effects of almost only positive $\Delta 1$ values in group I/III are not yet considered in equation (3), compare Fig. 12-I and 12-III. Furthermore, independence of adjacent screws is a strongly simplifying assumption owing to similar wood properties in the critical area and similar insertion geometry in case of parallel oriented adjacent screws.

2.7. Conclusions

Based on insertion tests with 8 mm self-tapping and self-drilling wood screws in spruce glulam these conclusions are drawn:

- Deviations between the actual and planned screw axis depend on the insertion geometry. In unfavourable cases the magnitude amounts to 12% related to the insertion length. This maximum is covered by tests without pre-drilling and with a maximum insertion length of 340 mm.
- If the intended angle between screw axis and grain direction is considerably less than 90° , the actual screw axis tends to follow the grain direction.
- The mainly positive $\Delta 1$ deviations in placement I and particularly in placement II and III are likely also caused by insertion angles systematically less than the intended 45° . The reason for this systematic inaccuracy is supposed to lie in the insertion procedure using the wedge-shaped screw guides (cf. Trautz et al. 2007, p. 67).
- If the entry point of the screw tip coincides with the glue line, it seems to be unlikely that the axis of screws remains in the glue line. This may be explained by the tendency of a screw to proceed in the lamination with lower density.
- Considering placement imperfections the necessary space for a single screw is cone-shaped. A cone model is therefore proposed in order to determine minimum screw spacing. Due to limited experimental data, the formulation of the model is in a tentative stage.

So far, consequences for screw spacing requirements are:

- Using the proposed cone model minimum screw spacing can be estimated such that harmful contact between adjacent screws is avoided. The model applies to four common insertion geometries. So far, its application is restricted to 8 mm wood screws, to spruce glulam and to an insertion length of approximately 400 mm.
- Screw spacing requirements should be discussed against the background of unintended deviations and harmful contact.
- Requirements in Eurocode 5 and technical assessments should at least be checked, amended where necessary or a general note should be made in provisions that deviations have to be taken into account.
- The results of the study are being used for a research proposal covering open questions. Several issues to be examined concern the use of screw guides and their influence on the actual screw axis, wood species, connection principles, insertion lengths exceeding 340 mm, the influence of the screw diameter and other than the examined insertion geometries.

3. References

Frese M (2019): Density variations in beech LVL - influence on insertion moment and withdrawal capacity of screws. INTER/52-7-3, Tacoma, U.S.A

Frese M, Jordan M (2018): Deviations between planned and actual position of wood screws - consequences for minimum spacing. INTER/51-7-1, Tallinn, Estonia

prEN 14592:2017 Timber structures - Dowel-type fasteners - Requirements

EN 15737:2009 Timber structures - Test methods - Torsional resistance of driving in screws

EN 1382:2016 Timber structures - Test methods - Withdrawal capacity of timber fasteners

Hassan J, Eisele M (2015): BauBuche - Der nachhaltige Hochleistungswerkstoff. Bautechnik 92 Nr. 1, 40-45

Frese M, Blaß HJ (2018): Entwicklung von selbstbohrenden Schrauben für Laubholz höherer Dichte. Schlussbericht für die Öffentlichkeit (FKZ 031A437J), KIT

Tarkow H, Seborg R (1968): Surface Densification Of Wood. Forest Products Journal 18 No. 9, 104-107

Stieger J (2016): Experimentelle Arbeiten, theoretische Untersuchungen und statistische Betrachtungen zur Entwicklung einer selbstbohrenden Hartholzschraube. Masterarbeit, KIT (unpublished)

Walter R (2016): Analyse von unterschiedlichen Gewindeformen für selbstbohrende Hartholzschrauben. Bachelorarbeit, KIT (unpublished)

Trautz M, Koj C (2015): Laser-drilled guide holes for self-tapping screws - Installation and load bearing behaviour. Bautechnik 92, 403-411

EN 1995-1-1:2004 Eurocode 5: Design of timber structures – Part 1-1: General – Common rules and rules for buildings

Müller V (2017): [...] Untersuchungen zu Fachwerkträgern mit [...] Zugdiagonalen aus BauBuche. Bachelorarbeit, KIT Holzbau und Baukonstruktionen (unpublished)

Blaß HJ (2017): Selbstbohrende Schrauben und Systemverbinder - Stand der Technik und Herausforderungen. 23. Internationales Holzbau-Forum IHF

Blaß HJ, Krüger O (2010): Schubverstärkung von Holz mit Holzschrauben und Gewindestangen. Bd. 15 Karlsruher Berichte zum Ingenieurholzbau, KIT Scientific Publishing

Bejtka I, Blaß HJ (2005): Self-tapping screws as reinforcements in connections with dowel-type fasteners. CIB-W18/38-7-4

Jordan M (2017): Entwicklung und Erprobung eines Untersuchungsverfahrens zur Ermittlung von Lagetoleranzen selbstbohrender Holzschrauben. Bachelorarbeit, KIT Holzbau und Baukonstruktionen (unpublished)

Trautz M et al. (2007): Mit Schrauben bewehren - Selbstbohrende Vollgewindeschrauben als Verstärkung in Brettschichtholzträgern und zur Ausbildung von hochleistungsfähigen Verbindungen. Forschungsbericht 01/2007, Lehrstuhl für Tragkonstruktionen, RWTH Aachen